

Effect of Crystal Size on Acetone Conversion over SAPO-34 Crystals

Yuichiro Hirota · Yuichi Nakano · Kazuo Watanabe ·
Yoshiaki Uchida · Manabu Miyamoto ·
Yasuyuki Egashira · Norikazu Nishiyama

Received: 9 December 2011 / Accepted: 3 March 2012 / Published online: 16 March 2012
© Springer Science+Business Media, LLC 2012

Abstract Catalytic properties of the 75 nm and 0.8 μm -sized SAPO-34 crystals on acetone-to-olefins (ATO) reaction were compared. The 75 nm-sized crystals (nanocrystals) showed longer catalyst lifetime than 0.8 μm -sized crystals, and products selectivity was similar for the two SAPO-34 catalysts, as is the case in methanol-to-olefins (MTO) and dimethylether-to-olefins (DTO) reactions. The reaction site of ATO reaction over SAPO-34 was studied using coke-deposited SAPO-34 as catalysts whose pores are deactivated through the DTO reaction. The reason for longer catalyst lifetime of the nanocrystals in the ATO reaction must be a large surface area of the SAPO-34 nanocrystals, unlike in the case of the MTO and DTO reactions.

Keywords SAPO-34 zeolite · Acetone · Light olefins synthesis

1 Introduction

Isobutene, a light olefin, has attracted both industrial and academic interest in recent decades, as it is widely used as feedstock for a range of products including octane

enhancer additives, alkylation, polymers, and rubbers. Since methyl tert-butyl ether was found to contaminate ground water, isobutene has been used to produce alternative octane enhancing additives for gasoline, such as diisobutene.

Chang and Silvestri [1] first reported that isobutene could be formed from acetone in high selectivity over ZSM-5 zeolite at low conversions. Subsequently, a number of studies have been reported on the acetone conversion over ZSM-5 [2–12], zeolite Y [3, 4, 10], and zeolite β [13, 14]. It is found that zeolite Y is not particularly active for this reaction, whereas ZSM-5 demonstrates high activity but low selectivity to light olefins [3]. Recently, Tago et al. [11, 12] reported that a decrease in aromatics yield and an increase in light olefins yield were achieved using ZSM-5 whose acid sites near the external surface were deactivated. On the other hand, zeolite β demonstrated markedly an enhanced selectivity to isobutene and high selectivity could be achieved for high acetone conversion [13, 14]. These reports suggest that production of light olefins including isobutene from acetone is a highly potential process, because a large amount of acetone is obtained as a by-product in the cumene process.

Song et al. [15] investigated olefin synthesis from acetone (ATO reaction) over SAPO-34 catalysts. They focused on the reaction mechanism of ATO reaction over zeolite catalysts. Although a high selectivity to C_4 olefins was observed, the detailed study on selectivity and catalyst lifetimes were not performed.

In this study, the SAPO-34 crystals were used as catalyst and the effects of its crystal size on products distributions and catalyst lifetime were examined. We also studied the reaction site of ATO reaction over SAPO-34 using the coke-deposited SAPO-34 whose pores are deactivated through the dimethylether-to-olefins (DTO) reaction.

Y. Hirota · Y. Nakano · K. Watanabe · Y. Uchida ·
Y. Egashira · N. Nishiyama (✉)
Division of Chemical Engineering, Graduate School of
Engineering Science, Osaka University, 1-3 Machikaneyama,
Toyonaka, Osaka 560-8531, Japan
e-mail: nishiyama@cheng.es.osaka-u.ac.jp

M. Miyamoto
Department of Materials Science and Technology, Gifu
University, 1-1 Yanagido, Gifu 501-1193, Japan

2 Experiments

2.1 Synthesis of SAPO-34

75 nm and 0.8 μm -sized SAPO-34 crystals were synthesized by a dry gel conversion (DGC) and a hydrothermal synthesis (HTS) methods, respectively, as described elsewhere [16]. Boehmite (AlOOH), 85 wt% phosphoric acid (both from Wako Pure Chemical Industries Co.) and colloidal silica (LUDOX HS-40, Aldrich) containing 40 wt% of SiO_2 were used as sources of aluminum, phosphorous, and silicon, respectively. A 20 wt% aqueous solution of tetraethylammonium hydroxide (TEAOH, Wako Pure Chemical Industries Co.) was used as the structure directing agent. The molar ratios were 1.0 Al_2O_3 :1.0 P_2O_5 :0.3 SiO_2 :1.8 TEAOH:77 H_2O for the DGC method and 1.0 Al_2O_3 :1.0 P_2O_5 :0.6 SiO_2 :1.8 TEAOH:77 H_2O for the HTS method. The precursor solution was stirred for 24 h at 303 K.

For the DGC method, the precursor solution was dried at 363 K. The obtained dry gel was placed in a Teflon-lined stainless steel vessel and a small amount of water, a source of steam, was separately added to the vessel. Crystallization was conducted at 453 K for 24 h in both the methods. The products were rinsed with deionized water and finally calcined at 823 K for 6 h.

2.2 Synthesis of SAPO-34/Carbon Composite

SAPO-34 pores were selectively blocked by coke deposition through the DTO reaction. The DTO reaction over SAPO-34 catalysts was performed by using a fixed-bed reactor made of quartz glass (i.d. 4-mm) with a continuous-flow system under atmospheric pressure. The feed rate of dimethylether (DME) was 3.2 mmol h^{-1} , and the reaction temperature was 723 K. When the DME conversion was decreased below 3 %, the DTO reaction was stop. Coke-deposited SAPO-34 was put into a tubular heater in flowing N_2 and was heated at 973 K for 3 h.

2.3 Characterization of SAPO-34 and SAPO-34/Carbon Composite

The nitrogen adsorption isotherms were measured at 77 K using a Quantachrome AUTOSORB-1 instrument. Total surface areas were calculated by the Brunauer-Emmett-Teller (BET) method.

The Ammonia temperature programmed desorption (NH_3 -TPD) measurement was conducted by the following procedures. About 0.1 g of sample was pretreated in vacuum at 773 K for 1 h and was subsequently cooled to the adsorption temperature of 373 K. Gas mixture of NH_3 and He (1 vol% of NH_3) was introduced into the sample cell

for 1 h. Subsequently, the He (60 ml-STP min^{-1}) was passed through the sample to remove weakly adsorbed NH_3 for 1 h. Then, the sample was heated up to 973 K at the rate of 10 K min^{-1} . Desorbed NH_3 signal was recorded on a Pfeiffer Vacuum Omnistar quadrupole GSD301 mass spectrometer.

The amount of carbon deposition was measured by a Shimadzu DTG-50 thermogravimetry (TG) in a static air atmosphere with a heating rate of 5 K min^{-1} . The carbon deposition was calculated from the mass ratio of 573 K to 1,073 K.

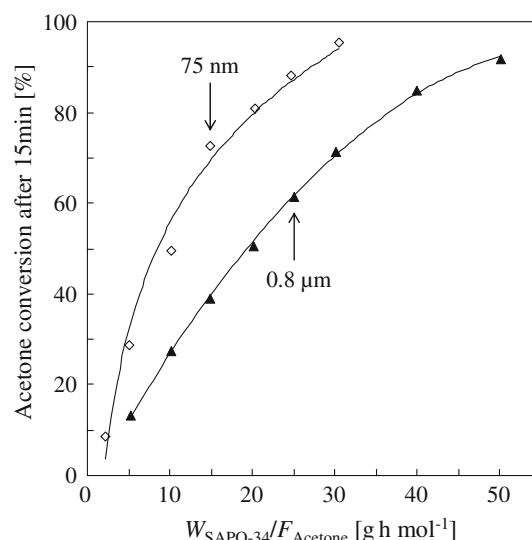


Fig. 1 Changes of acetone conversion after 15 min with $W_{\text{SAPO-34}}/F_{\text{Acetone}}$

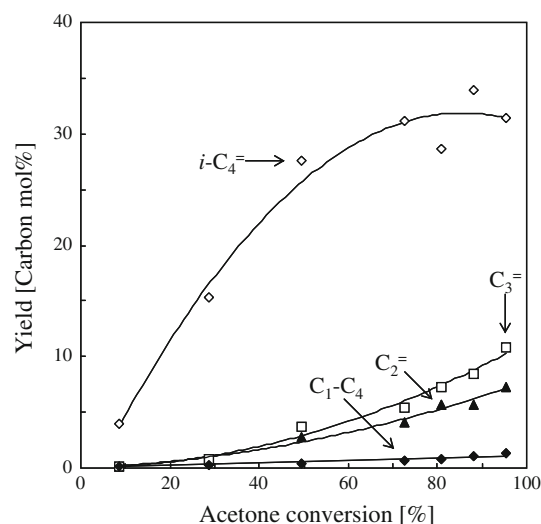
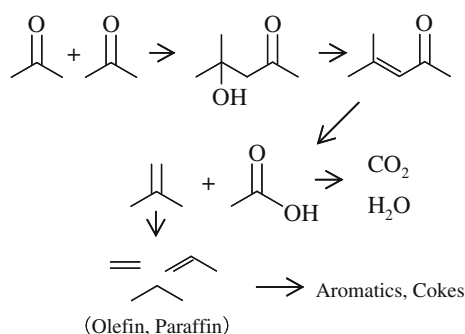


Fig. 2 Changes of yield of gas components as a function of acetone conversion over 75 nm-sized SAPO-34 catalysts



Scheme 1 Reaction pathways for light olefins synthesis from acetone over solid acid catalysts

2.4 Catalytic Testing

Acetone conversion over SAPO-34 crystals was performed by using a fixed-bed reactor made of quartz glass (i.d. 4-mm) with a continuous-flow system under atmospheric pressure. The feed rate of acetone was 2.5 mmol h^{-1} , the partial pressure of acetone was 9.45 kPa and the reaction temperature was 773 K. The value of $W_{\text{SAPO-34}}/F_{\text{Acetone}}$

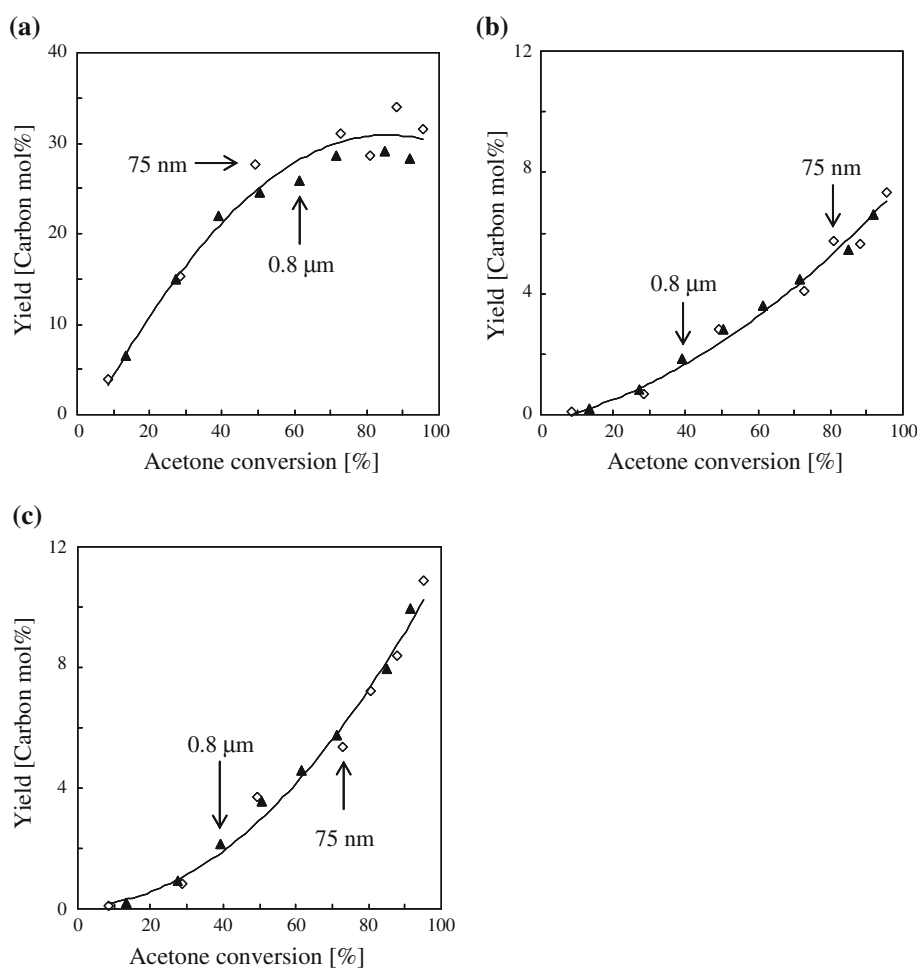
(mass of SAPO-34 crystals (g) divided by the feed rate of acetone (mol h^{-1})) was set up from 2.5 to 50, by changing $W_{\text{SAPO-34}}$ (the value of WHSV ($g_{\text{Acetone}} g_{\text{SAPO-34}}^{-1} \text{h}^{-1}$) was from 1.2 to 23 at 300 K). The product stream after 15 min was analyzed with a Shimadzu GC-14B gas chromatograph equipped with a flame ionization detector using GS- Al_2O_3 PLOT column (J&W scientific) and a Shimadzu GC-8A gas chromatograph equipped with thermal conductivity detector using Porapak Q column (Shinwa Chemical Industries, Ltd.).

3 Results and Discussions

3.1 Acetone Conversion over Fresh SAPO-34 Catalysts

Acetone conversion over 75 nm and $0.8 \mu\text{m}$ -sized SAPO-34 catalysts was carried out in order to investigate the effect of crystal sizes on product distributions and catalyst lifetime. The conversions after 15 min are plotted as a function of $W_{\text{SAPO-34}}/F_{\text{Acetone}}$ in Fig. 1. The 75 nm-sized SAPO-34 showed a higher conversion and a longer

Fig. 3 Changes of yield of (a) isobutene, (b) ethylene, and (c) propylene as a function of acetone conversion



catalysts lifetime than 0.8 μm -sized crystals at the same $W_{\text{SAPO-34}}/F_{\text{Acetone}}$, as is the case in the methanol-to-olefins (MTO) and DTO reactions [16]. This result indicates that coke deposition is slower on smaller SAPO-34 crystals.

Yields of gas components (isobutene, ethylene, propylene, and $\text{C}_1\text{--C}_4$ saturated alkane) are plotted as a function of acetone conversion over 75 nm-sized catalysts in Fig. 2. Isobutene was selectively formed from acetone. Scheme 1 shows possible reaction pathways for light olefins synthesis from acetone over solid acid catalysts [14, 15]. Isobutene was first produced from aldol condensation products of acetone, followed by production of propylene, ethylene, and aromatics over acid sites. Isobutene is an intermediate chemical in the series of reactions with aromatics and coke as terminal products. Isobutene yield reached a maximum at the acetone conversion of 80–90 %, and was decreased with increasing conversion. The obtained relationships between isobutene yields and acetone conversion agree with the reaction mechanism shown in Scheme 1.

Yields of isobutene, ethylene, and propylene of 75 nm-sized catalysts are compared to those of 0.8 μm -sized crystals in Fig. 3. The relationships between product yield and acetone conversion over both the SAPO-34 catalysts were similar, indicating that product distributions were not affected by the size of SAPO-34 crystals.

3.2 ATO Reaction over SAPO-34/Carbon Composite Catalysts

The SAPO-34 nanocrystals showed a longer catalyst lifetime than 0.8 μm -sized crystals. The possible reasons for longer catalyst lifetime of the nanocrystals are differences in (1) the catalyst effectiveness factor and (2) the external surface area. To investigate the reaction site of acetone

conversion over SAPO-34, selective coke deposition within the pores of SAPO-34 nanocrystals via the DTO reaction was applied for examination of the reaction site over the SAPO-34 catalysts. The SAPO-34 cage like pores can be blocked by the coke depositions through the MTO and DTO reactions [16].

From the TG analysis, the amount of carbon deposited on the SAPO-34 nanocrystals was a 23 wt% of the mass of SAPO-34 crystals. The BET surface areas of SAPO-34 nanocrystals were decreased from 590 to 90 m^2/g after the carbon depositions, indicating that the SAPO-34 cage like pores were almost fully filled with carbon, because the external surface area of the 75 nm-sized SAPO-34 is calculated to be 45 m^2/g . The NH_3 -TPD profiles of SAPO-34

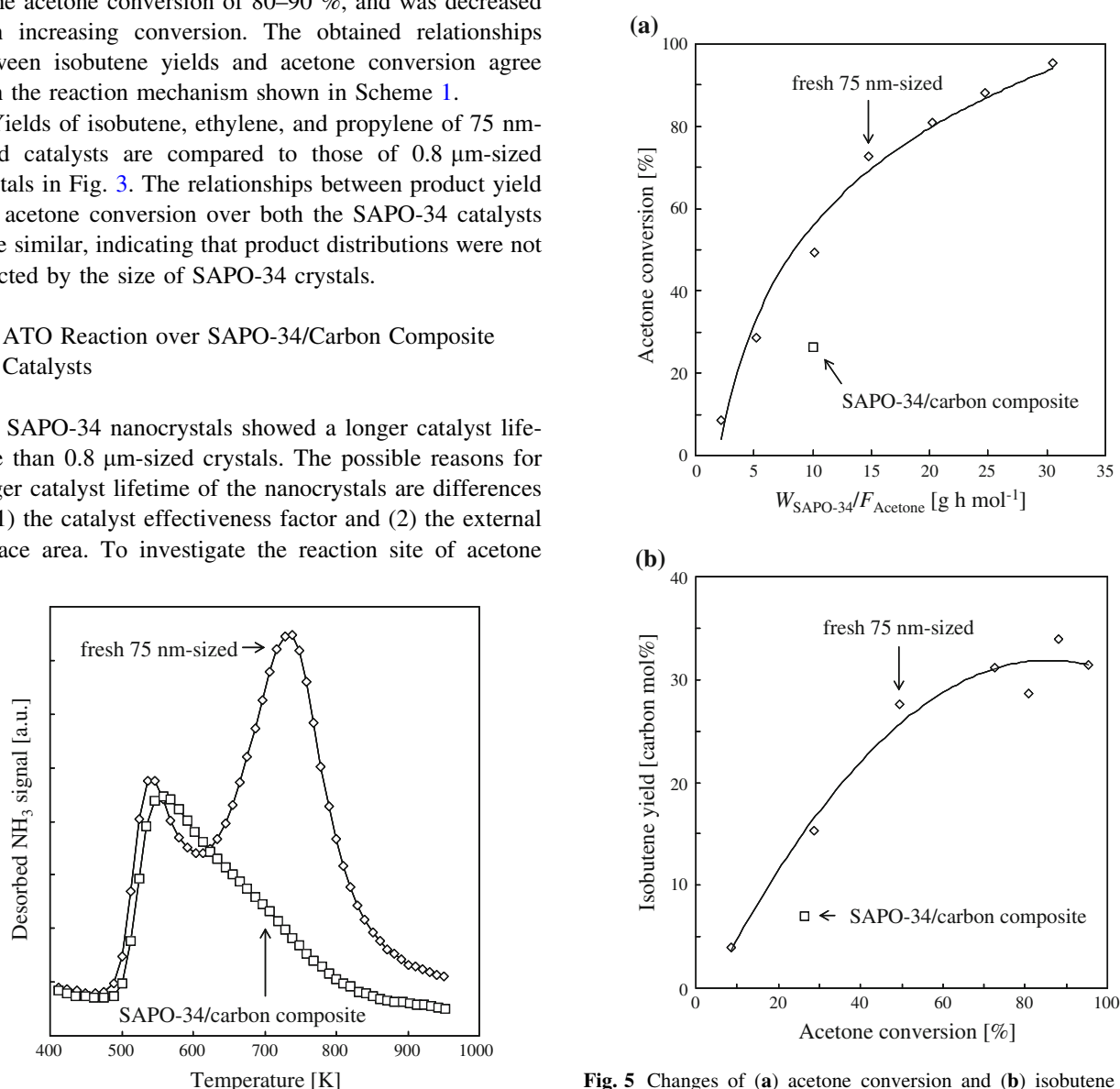


Fig. 4 NH_3 -TPD profiles of 75 nm-sized SAPO-34 catalysts

Fig. 5 Changes of (a) acetone conversion and (b) isobutene yield after 15 min as a function of $W_{\text{cat}}/F_{\text{Acetone}}$ over 75 nm-sized SAPO-34 catalysts

nanocrystals before and after carbon depositions were shown in Fig. 4. There are two desorption peaks at 500–610 K and 610–900 K for SAPO-34 nanocrystals before carbon depositions, which correspond to the weak acid sites and strong acid sites, respectively. The peak intensity for the strong acid sites decreased after carbon depositions, whereas the desorption peak for weak acid sites was not changed so much. The results indicate that the strong acid sites in SAPO-34 pores must have been deactivated by carbon depositions.

Acetone conversion and isobutene yield of SAPO-34/carbon composite catalysts are plotted in Fig. 5. Acetone was converted into isobutene over SAPO-34/carbon composite catalysts, although this catalyst shows no active for the DTO reaction. The result indicates that the reaction proceeded mainly on the outer surface of SAPO-34. Although the DTO reaction proceeds in SAPO-34 pores, part of acid sites on the outer surface might be also deactivated by coke deposition. Decrease of acetone conversion and isobutene yield might be due to a difference in number of acid site on the outer surface. These results indicate that the reason for longer catalyst lifetime of the nanocrystals in the acetone conversion is a large external surface area of the SAPO-34 nanocrystals unlike in the case of the MTO and DTO reactions.

4 Conclusions

The SAPO-34 nanocrystals showed a longer catalyst lifetime than 0.8 μm -sized crystals in the acetone conversion, as is the case in the MTO and DTO reactions. Isobutene was formed from acetone over both SAPO-34 catalysts. The relationships between yields of light olefins and acetone conversion over both the SAPO-34 catalysts were similar, indicating that product distributions were not related to the size of SAPO-34 crystal.

Selective coke deposition within the pores of SAPO-34 nanocrystals via the DTO reaction was applied for examination of the reaction site over the SAPO-34 catalysts. Acetone was converted into isobutene over SAPO-34/carbon composite catalysts, indicating that the reaction proceeded mainly on the outer surface of SAPO-34 crystals. The reason for longer catalyst lifetime of the nanocrystals in the acetone conversion must be a large surface area of the SAPO-34 nanocrystals, unlike in the case of the MTO and DTO reactions.

References

1. Chang CD, Silvestri AJ (1997) *J Catal* 47:249
2. Nováková J, Kubelková L, Dolejšek Z (1987) *J Mol Catal* 39:195
3. Kubelková L, Čjka J, Nováková J, Boszáček V, Jirka I, Jíaru P (1989) *Stud Surf Sci Catal* 49:1203
4. Boszáček V, Kubelková L, Nováková J (1991) *Stud Surf Sci Catal* 65:337
5. Kubelková L, Čjka J, Nováková J (1991) *Zeolite* 11:48
6. Dolejšek Z, Nováková J, Boszáček V, Kubelková L (1991) *Zeolite* 11:244
7. Kubelková L, Nováková J (1991) *Zeolite* 11:822
8. Biaglow AI, Sepa J, Gorte RJ, White D (1995) *J Catal* 151:373
9. Panov AG, Fripiat JJ (1998) *J Catal* 151:188
10. Panov A, Fripiat JJ (1998) *Lamgmuir* 14:3788
11. Tago T, Sakamoto M, Iwakai K, Nishihara H, Mukai SR, Tanaka T, Masuda T (2009) *J Chem Eng Jpn* 42:162
12. Tago T, Konno H, Sakamoto M, Nakasaka Y, Masuda T (2011) *Appl Catal A: Gen* 403:183
13. Hutchings GJ, Johnston P, Lee DF, Williams CD (1993) *Catal Lett* 21:49
14. Tago T, Konno H, Ikeda S, Yamazaki S, Ninomiya W, Nakasaka Y, Masuda T (2011) *Catal Today* 164:158
15. Song W, Nicholas JB, Haw JF (2001) *J Phys Chem B* 105:4317
16. Hirota Y, Murata K, Miyamoto M, Egashira Y, Nishiyama N (2010) *Catal Lett* 140:22